



Molecular dynamics simulation of material removal process and mechanism of EDM using a two-temperature model



Xiaoming Yue^{a,b,c}, Xiaodong Yang^{d,*}

^a Key Laboratory of High Efficiency and Clean Mechanical Manufacture, Ministry of Education, Shandong University, Jinan 250061, China

^b School of Mechanical Engineering, Shandong University, Jinan 250061, China

^c Suzhou Research Institute, Shandong University, Suzhou 215123, China

^d Department of Mechanical Engineering and Automation, Harbin Institute of Technology, Harbin 150001, China

ARTICLE INFO

Keywords:

Electrical discharge machining (EDM)
Molecular dynamics (MD) simulation
Two-temperature model (TTM)
Heat conduction
Denatured layer

ABSTRACT

Molecular dynamics (MD) simulation has been used to investigate the material removal mechanism in electrical discharge machining (EDM). However, in the previous researches, the simulation model was too small, and the effect of free electrons on the heat conduction has not been considered. To solve the above two problems, in this study, a 2-D sub-micrometer scale simulation with a two-temperature model (TTM) was conducted to simulate the discharge process of EDM, which can consider the effect of both the lattice vibration and free electrons on the heat conduction simultaneously. This 2-D sub-micrometer scale simulation model based on TTM has successfully obtained a sub-micrometer scale discharge crater which was close to the smallest discharge crater reported. Furthermore, the simulation result demonstrates that the pressure generated inside the molten pool serves as one of the removal mechanisms of molten material in the discharge process of EDM. In addition, compared with the monocrystal copper, discharge on the polycrystalline copper can generate much more defect structures and larger denatured layer. Moreover, the smaller the grain size of polycrystalline copper, the more the defect structures and the larger the denatured layer will be.

1. Introduction

Electrical discharge machining (EDM) is a kind of thermal machining methods in which workpiece materials can be removed through the melt and evaporation by the discharge plasma. Thus, EDM has been widely applied in the manufacturing industry because of its excellent property of using heat to process most of electrically conductive material regardless of hardness. However, traditionally, it is quite difficult to experimentally investigate the discharge process of EDM because the discharge process in EDM happens in an extremely short time (tens of nanoseconds ~ hundreds of microseconds) and narrow space (several micrometers ~ tens of micrometers) [1]. As a result, until now, many discharge phenomena in EDM, such as the material removal process, material removal mechanisms, etc, have not been explained and clarified thoroughly, which seriously hinders the further improvement of EDM technology. With the rapid development of numerical calculation method and computer technology, complex simulation of thermal machining process is becoming a reality. Thereby, nowadays, study on single discharge process through the numerical calculation method is the most direct and easiest way to understand the microscopic process

and mechanism of EDM. At present, many researchers use the finite element method (FEM) to investigate single discharge process in EDM [2–4]. In their studies, the temperature fields inside the workpiece material caused by the discharge heat were computed successfully, then, based on the simulation result of temperature distribution, the discharge process was investigated. However, in the above studies, the dynamics behavior of material was not considered such as the melting and solidification process, thus, revealing and explaining the material removal process and mechanism during a single discharge of EDM only by calculating the temperature distribution inside the electrode material is impossible. Although some researchers have simulated the material removal in single discharge process by using FEM [5], only the evaporation removal of material was considered while the melt removal of material was not taken into account. Because in the governing equation of this simulation, only the source term of evaporation process was calculated while the source term of melt process was ignored. Thereby, the removal mechanism of molten material in EDM, which is the most essential material removal mechanism of EDM, still cannot be clarified through the above simulation. Moreover, FEM can't investigate the formation and evolution of the defect structures during the

* Corresponding author.

E-mail address: xdyang@hit.edu.cn (X. Yang).

discharge process from atomic level.

Molecular Dynamics (MD) simulation is a numerical simulation technique for computing the trajectory and interaction of atoms and molecules based on the Newton's law, which provides an effective method to analyze simultaneously mechanical and thermal behavior of material in an atomic scale. Thus, MD simulation has been used in the research of materials [6], biology [7], mechanical machining [8], etc. In recent years, applications of MD simulation in EDM have been reported. Shimada et al. studied the microscopic mechanism of self-sharpening phenomenon of thin tungsten electrodes in single discharge process by using the MD simulation [9]. Yang et al. realized the establishment of simulation model of discharge process and applied the Gaussian heat source on the simulation model [10,11], then, based on the above MD simulation model, they investigated the material removal process, the stress distribution in the electrode material, and the removed materials distribution. Also, Yue et al. studied the evolution process of crystal structures of electrode material and the formation of the bubble in the discharge process by using the MD simulation [12–14]. From the above research results, it can be known that through the MD simulation, not only the melting and solidification process of the electrode material, but also the formation process of denatured layer of the electrode material in the discharge process can be simulated and investigated. However, in the previous studies [9–14], all the simulation models only considered the heat conduction caused by lattice vibration while the heat conduction caused by free electrons is neglected. Since in the metal materials, the free electrons play a significant role in the heat conduction, thus, neglecting its influence can result in large calculating error in the temperature distribution. Zhang et al. innovatively studied the machining process of nano-electrical discharge machining based on combined atomistic-continuum modeling method, which considered both the lattice vibration and free electrons in the heat conduction successfully [15]. However, the spatiotemporal scale of the simulation is still small, but this study provides an excellent research ideal to study the material removal mechanism of EDM by MD method with considering both the lattice vibration and free electrons in the heat conduction.

Therefore, this study uses a 2-D sub-micrometer scale model coupled the two-temperature model (TTM) to simulate the discharge process of EDM. The above two-temperature model can consider the influence of both the lattice vibration and free electrons on the thermal conduction simultaneously. Then, the melt, evaporation, removal and solidification of workpiece material in the discharge process were simulated and investigated. Finally, the material removal mechanism and the formation of denatured layer were investigated and clarified.

2. Simulation model and computational details

2.1. Simulation model

It is common knowledge that MD simulation costs computer resources extremely. Thus, limited by the computational capacity, in previous researches [10–14], the MD simulation model was just tens of nanometers scale, which was too small even compared with the smallest discharge crater in micro EDM [16,17]. To enlarge the simulation model, a 2-D sub-micrometer scale model was adopted to obtain a sub-micrometer scale discharge crater, as shown in Fig. 1. Firstly, a 3-D model with the dimension of 250 nm × 125 nm × 250 nm (as shown in the left part of Fig. 1) was cut into 2-D slices with the thickness of 2 nm (as shown in the right part of Fig. 1). Then, the periodic boundaries were applied on the two sides of the 2-D model, as shown in the right part of Fig. 1. Based on the theory of MD simulation, the periodic boundary means that in this 2-D model, atoms can interact across the boundary, that is, they can exit one side of the 2-D model and re-enter the other side of the 2-D model as if both the sides of the 2-D model have another 2-D model. Thus, we can investigate the discharge process of the above 3-D model through this 2-D model which is actually a local

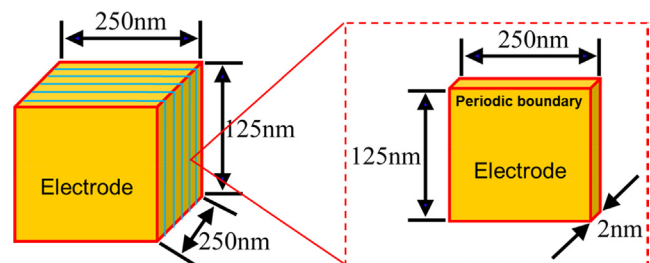


Fig. 1. Schematic diagram of 3-D model (left) and 2-D model (right).

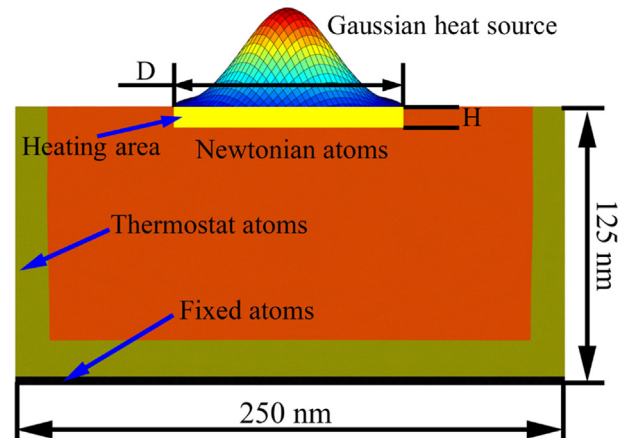


Fig. 2. MD simulation model.

area of this 3-D model. The above simplification can save the computer resources tremendously. For example, the above 3-D model contains about 661,492,792 atoms while this 2-D model only has about 5,291,942 atoms. Thereby, this 2-D model provides a simpler way to enlarge the simulation scale without using much stronger computer sources.

Fig. 2 shows the simulation model in which the electrode is 250 nm wide, 125 nm high and 2 nm thick. To fix the simulation model, the fixed atoms layer with the thickness of 5 nm were used at the bottom of the model, in which the velocity of fixed atoms were always forced to be zero in the whole simulation process. Then, in order to guarantee an adequate heat transfer, the thermostat atoms layer with the thickness of 20 nm were distributed between the fixed atoms layer and Newtonian atoms layer. The atoms in the Newtonian atoms layer follow the Newton's law. In the machining process of EDM with the dielectric liquid, the bubble formed around the discharge spot, and the material removal happened in the bubble actually [18]. Thus, for simplicity, the discharge gap was set to be vacuum in the simulation model. Also, the initial temperature of simulation model was set to be 300 K. The simulation was conducted by using a large-scale atomic/molecular massively parallel simulator (Lammps) [19]. For metals in lammps, the units are shown as follows: mass = grams/mole, distance = Angstroms, time = picoseconds, energy = eV, velocity = Angstroms/picosecond, force = eV/Angstrom, temperature = Kelvin.

2.2. Interatomic force field

MD simulation calculates the trajectory and interaction of atoms based on the Newton's law. An accurate force field, which can describe the interaction among atoms, is the most important foundation for MD simulation. In this study, copper material was used as the electrode, thus, a three-body Embedded-Atom Method (EAM) potential was used to describe the interaction among copper atoms [20]. In this potential function, the total atomic potential energy in the system is given by Eq.

(1).

$$E_{tot} = \sum_i \left[F_i(\rho_i) + \frac{1}{2} \sum_{i \neq j} \phi_{ij}(r_{ij}) \right] \quad (1)$$

here, ϕ_{ij} is pair-interaction energy between atoms i and j , and F_i is embedded energy of atom i . r_{ij} is distance between atoms i and j . ρ_i is host electron density at atom i due to the remaining atoms in the system, which can be described by Eq.(2).

$$\rho_i = \sum_{i \neq j} \rho_j(r_{ij}) \quad (2)$$

Through the interatomic force field, the movement of atoms based on the Newton's law can be calculated, as shown by Eq. (3).

$$\begin{cases} m_i \frac{d^2 \vec{r}_i(t)}{dt^2} = \vec{F}_i(t) \\ \vec{F}_i(t) = -\frac{\partial E_{tot}}{\partial \vec{r}_i} \end{cases} \quad (3)$$

here, m_i is the mass of atom i , \vec{F}_i is force vector acted on atom i , and \vec{r}_i is the position vector of atom i .

2.3. Heat source description of discharge plasma

In an actual discharge process, the discharge plasma, which is composed of ions, electrons, and neutral atoms, completes expanding rapidly after the electric breakdown of the dielectric. After that, the diameter of the discharge plasma keeps stable [21]. In this study, for simplicity, the formation and expansion of the plasma were not considered and the compositions of the plasma were also ignored. Thus, the heat source, which is actually the discharge plasma can be simplified and described through a mathematical model of Gaussian heat source with a constant diameter, which is a widely used heat source in the simulation of EDM, described by Equation (4).

$$P(r) = P_m \exp(-kr^2) \quad (4)$$

here, r is the distance from the center of the arc column, $P(r)$ is the discharge power given to an atom located at radius r , P_m is the discharge power at $r = 0$, k is the heat source concentration factor.

In the MD simulation of discharge process, the Gaussian heat source is exerted on the heating area, which is a rectangle with the width D and height H , as shown in Fig. 2. That is, only the atoms in this heating area can gain discharge energy in the whole simulation process.

2.4. Two-temperature model

In the metal materials, the heat can be transferred through both the lattice vibration and thermal movement of free electrons. However, limited by the simulation algorithm and computational capacity, in the previous studies [9–13], the influence of the free electrons on the heat conduction was neglected, and only the heat conduction by the lattice vibration was considered, which didn't accord with the reality. Thus, to resolve the above shortcoming, in this study, a two-temperature model (TTM), which can consider the influence of both the lattice vibration and free electrons on the thermal conduction simultaneously, was used to simulate the discharge process of EDM. The basic principle of this TTM model was shown as follows [22].

The schematic diagram of TTM can be explained by Fig. 3, which consists of two subsystems: the atomic subsystem and the electronic subsystem. The atomic subsystem is actually a molecular dynamics model, but the electronic subsystem is modelled as a continuum, or a background “gas”, on a regular grid. Heat can be transferred spatially within the grid representing the electrons. Heat can also be transferred between the electronic and the atomic subsystems.

The atomic subsystem is described by Equation (5), which is a standard MD equation shown by Equation (3) adding a Langevin

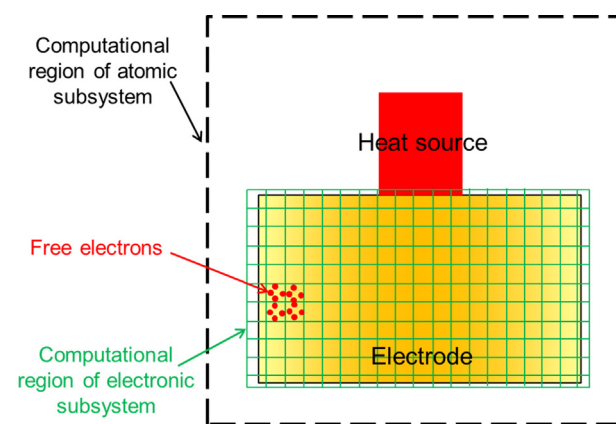


Fig. 3. Schematic diagram of two-temperature model (TTM).

thermostat item. The velocity (\vec{v}_i) of atoms i (mass m_i) is subjected to a force (\vec{F}_i) due to the interactions with the surrounding atoms. The Langevin thermostat item $\gamma_p \vec{v}_i$ represents the energy exchange by electron-atom interactions. γ_p is the adjustment coefficient of atoms velocity after exchanging energy between atomic subsystem and electronic subsystem.

$$m_i \frac{\partial \vec{v}_i}{\partial t} = \vec{F}_i(t) - \gamma_p \vec{v}_i \quad (5)$$

The electronic subsystem is described by the heat diffusion equation shown by Equation (6), which can be computed through cutting the subsystem region into many grid cells shown in Fig. 3.

$$C_e \frac{\partial T_e}{\partial t} = \nabla(\kappa_e \nabla T_e) - g_p(T_e - T_a) \quad (6)$$

here, $C_e = 3.3868 \times e^{-7} \text{ eV}/\text{\AA}^3 \times K$ is the electronic specific heat at 300 K, $\kappa_e = 6.5 \times 10^{-3} \text{ eV}/\text{ps} \times K \times \text{\AA}$ is the electronic thermal conductivity at 300 K, T_e and T_a are the local electronic temperature and the effective local atomic temperature, g_p is the represent energy exchange coefficient with the lattice via electron-ion interactions.

The atomic subsystem and the electronic subsystem are linked together to transfer the energy through the Equation (7).

$$g_p = \frac{3Nk_B\gamma_p}{\Delta V m} \quad (7)$$

here, $\Delta V = 28920 \text{\AA}^3$ is the volume of the grid cell in Fig. 3, $N = 2448$ is the number of atoms in the grid cell, $k_B = 0.8629055 \times 10^{-4} \text{ eV}/\text{K}$ is the Boltzmann constant, $m = 64 \text{ g/mol}$ is the atom mass, $\gamma_p = 1.92 \text{ g/mol} \times \text{ps}$ is the adjustment coefficient of atoms velocity after exchanging energy between atomic subsystem and electronic subsystem [22].

The above TTM can be achieved by the command of ‘Fix TTM’ in the Lammps software. In practice, all the material properties are temperature dependent. However, the above parameters of the material properties in this command are taken as constant values for simplicity [19].

3. Simulation results and discussions

3.1. Temperature distribution of electrode material

The MD simulation of temperature distribution was implemented in the lammps software with the discharge time of 0.5 ns and the total simulation time of 1 ns. The material of simulation model used is a monocrystal copper. The dimension of the heating area in the simulation model was 100 nm wide and 50 nm height. In the Gaussian heat source, the discharge power P_m at $r = 0$ was 0.4 GeV/ps.

Fig. 4 shows the temperature field inside the electrode material, which was colored by the temperature bar shown in the right part of

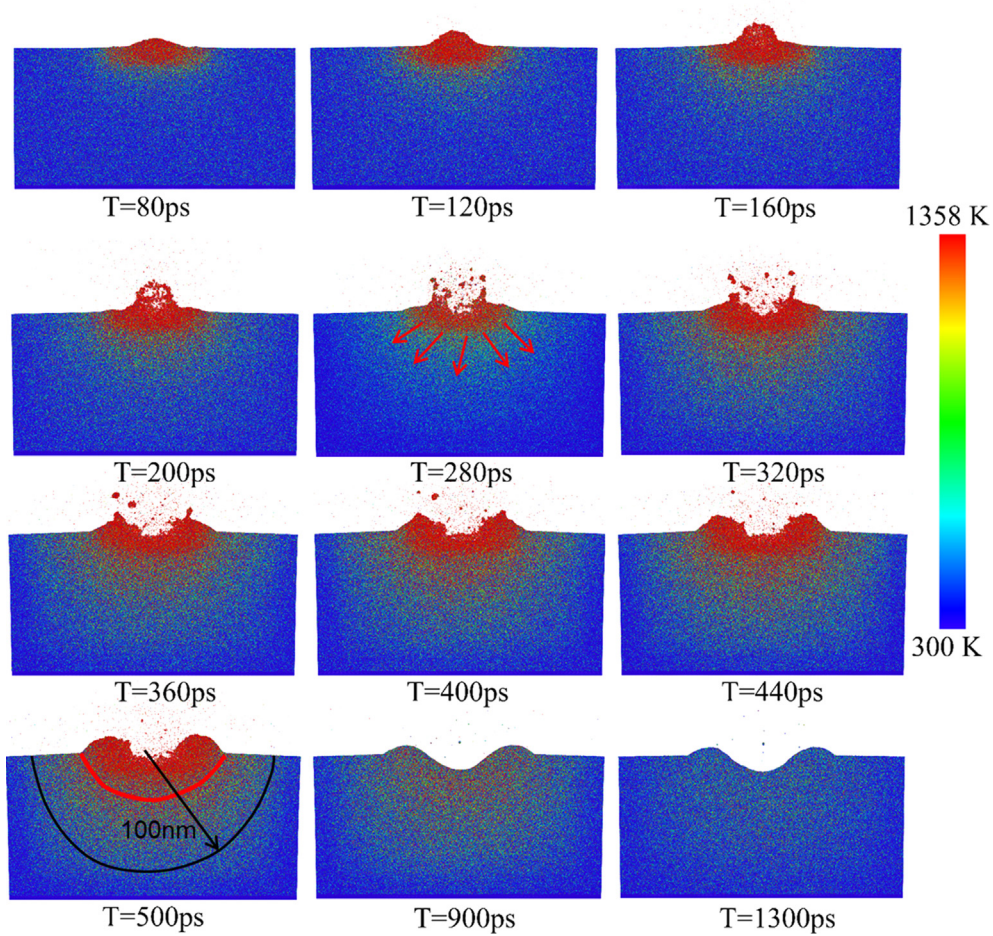


Fig. 4. Temperature distribution of electrode material.

Fig. 4 through calculating the kinetic energy of atoms. From the figure, it can be found that after the discharge was ignited ($t > 0$ ps), the electrode material was heated by the discharge energy, and the temperature of electrode material around the discharge spot increased largely. At the initial stage of discharge, such as the moment at 80 ps, the electrode material around the discharge spot reached the melting point quickly. As the discharge went on, continuously input by the discharge energy, the high-temperature area around the discharge spot enlarged and the temperature of electrode material far away from the discharge spot also went on increasing due to the heat transfer through both the lattice vibration and thermal movement of free electrons, such as the moment at 280 ps. When the discharge ended, the transferring range of the discharge heat can be 100 nm, as shown at $t = 500$ ps. After the end of discharge ($t > 500$ ps), the electrode material cooled and its temperature decreased gradually. Actually, we also tried to simulate this discharge process only considering the heat conduction by the lattice vibration, however, the simulation failed. Because most of the discharge energy concentrated around the discharge spot and can't be transferred inside the electrode in the discharge process since in the metal materials, the free electrons play a more important role in transferring the heat than the lattice vibration. As a result, the material temperature around the discharge spot was extremely high and beyond the calculating capacity of the lammps software. Thus, the failing simulation demonstrated that considering both the lattice vibration and free electrons is much closer to the actual situation.

Fig. 5 shows the morphology of discharge crater after the end of discharge. From the figure, it can be found that this sub-micrometer scale MD model based on TTM has successfully obtained a sub-micrometer scale discharge crater whose diameter and depth were 132 nm

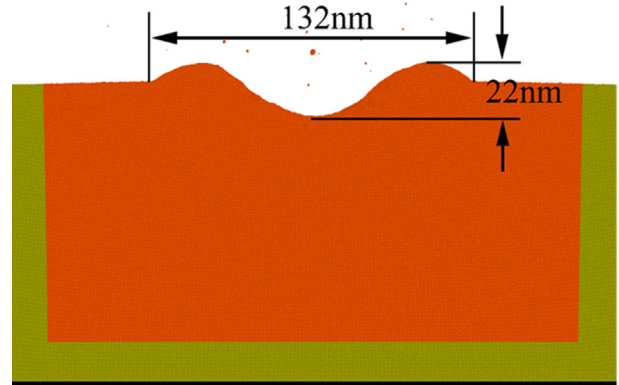


Fig. 5. Morphology of discharge crater formed in single discharge.

and 22 nm, respectively. The dimensional scale of this discharge crater was close to the smallest discharge crater reported [17]. The bulge around the discharge crater was also similar to that of the discharge crater in micro EDM, which indicates that this sub-micrometer MD model based on TTM can simulate the discharge process of EDM more truly compared with the previous models [10,11].

3.2. Material removal mechanism and forming process of denatured layer

To distinguish the state of lattice, a kind of computation that calculates the centro-symmetry parameter for each atom in the group, called centro-symmetry parameter (CSP) [23], was employed. The

centro-symmetry parameter can be used to analyze the local lattice disorder around an atom, which was described by the following equation:

$$CSP = \sum_{i=1}^{N/2} |\vec{R}_i + \vec{R}_{i+N/2}|^2 \quad (8)$$

Here, the N nearest neighbors are identified and R_i and $R_{i+N/2}$ are vectors from the central atom to a particular pair of nearest neighbors. N is an input parameter, as for the Face Centered Cubic (FCC), N is set to 12. For an atom on a lattice site, surrounded by atoms on a perfect lattice, the centro-symmetry parameter will be 0. It will be near 0 for small thermal perturbations of a perfect lattice. If a point defect exists, the symmetry is broken, and the parameter will be a larger positive value. Thus, we can use the CSP of an atom to identify the local disorder of one atom and the type crystal defects. In this simulation, the atoms whose CSP value was less than three were colored yellow while the atoms whose CSP value was more than three were colored red. Especially, the yellow atoms ($CSP < 3$) in the simulation model stood for the perfect lattices or near perfect lattices. Before the discharge, the red atoms ($CSP > 3$) in the simulation model stood for the grain boundary of the crystalline grain. During the discharge, the red atoms ($CSP > 3$) in the simulation model stood for the disordered state atoms caused by the fierce thermal motion of atoms. After the discharge, the red atoms ($CSP > 3$) in the simulation model stood for the grain boundary of the crystalline grain or the defect structures.

Fig. 6 shows the MD simulation of the discharge on a monocrystal copper. The total discharge time and simulation time were 0.5 ns and 2 ns, respectively. The dimension of heating area in the simulation model was 150 nm wide and 75 nm height. In the Gaussian heat source, the discharge power P_m at $r = 0$ was 1.4 GeV/ps.

At the initial stage of discharge ($t < 140$ ps), there was no large amount of removed material but small amount evaporating material. As the discharge went on, at the moment of $t = 200$ ps, the removal of large molten material happened. Along with massive removal of

electrode material around the discharge spot, the discharge crater formed and the bulge around the discharge crater was generated gradually. After the end of discharge ($t > 900$ ps), the discharge crater and bulge were formed steadily. In the whole discharge process, it can be found that at the initial stage of the discharge process, the molten pool swelled slightly, which displayed the material removal tendency. Then, as the discharge time went on, the swell went on expanding and at the moment of $t = 200$ ps, the swell broke open and large amount of molten material was removed.

The above phenomenon shows that these must exist in some sort of force inside the molten pool and this force can help molten materials get rid of the attraction among atoms and break away from the electrode. As has been explained in **Fig. 4**, after the discharge was ignited, the discharge energies were transferred into the materials continuously, resulting in temperature rise of materials around the discharge spot. As the discharge continued, the accumulated heat led to the melt and evaporation of materials around and under the discharge surface. Then, evaporating materials inside the molten pool resulted in high pressure inside the molten pool, which made the molten pool expand outward and the swell was formed (forming process of swell), as shown at the moment of $t = 200$ ps. When the pressure inside molten pool exceeded the binding force among atoms, the swell broke open and the molten material started to depart from the electrode surface (blasting process of swell). From **Fig. 6**, it can also be found that at the initial time of discharge, large numbers of materials around the discharge spot reached the melting point, however, these materials were not removed largely happen until 200 ps. This is because before 200 ps, the pressure generated inside the molten pool was not large enough to overcome the binding force among atoms. Thereby, it can be concluded that the pressure generated inside molten pool serves as one of the removal mechanisms of molten material in the discharge process of EDM.

Figs. 7 and 8 show the MD simulation of the discharges on the polycrystalline copper with the grain size of 15 and 10 nm, respectively. The discharge conditions were the same with these of the discharge shown in **Fig. 6**. The crystalline grain in the simulation model was

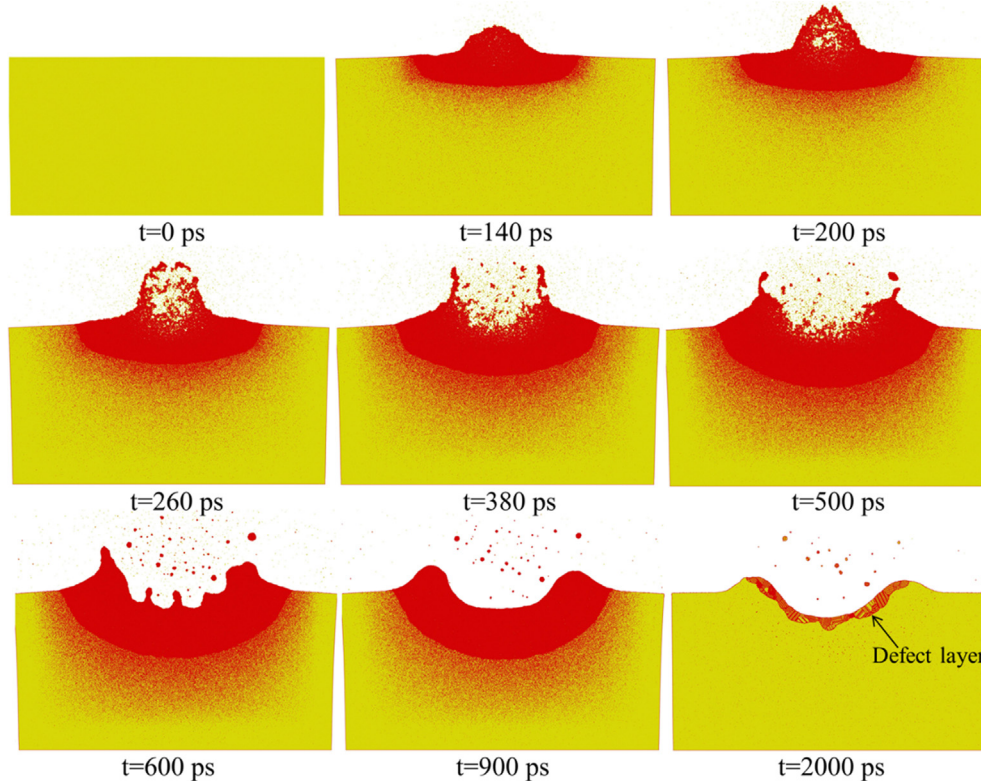


Fig. 6. Material removal process of monocrystalline copper.

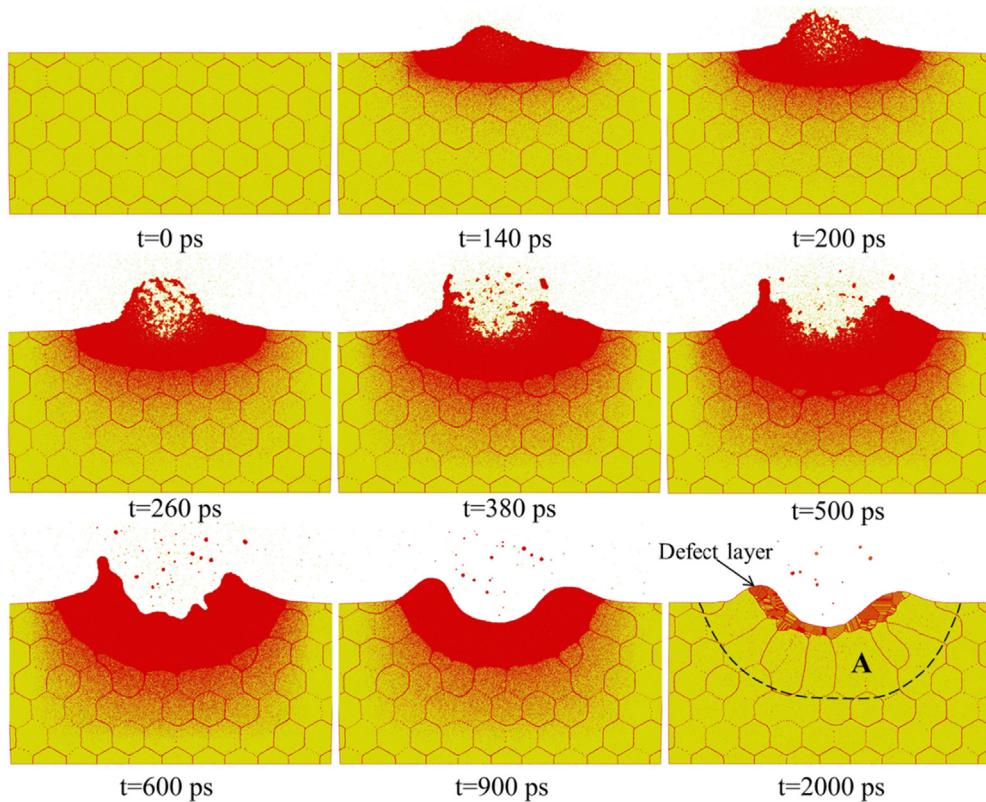


Fig. 7. Material removal process of polycrystalline copper with 15 nm grain size.

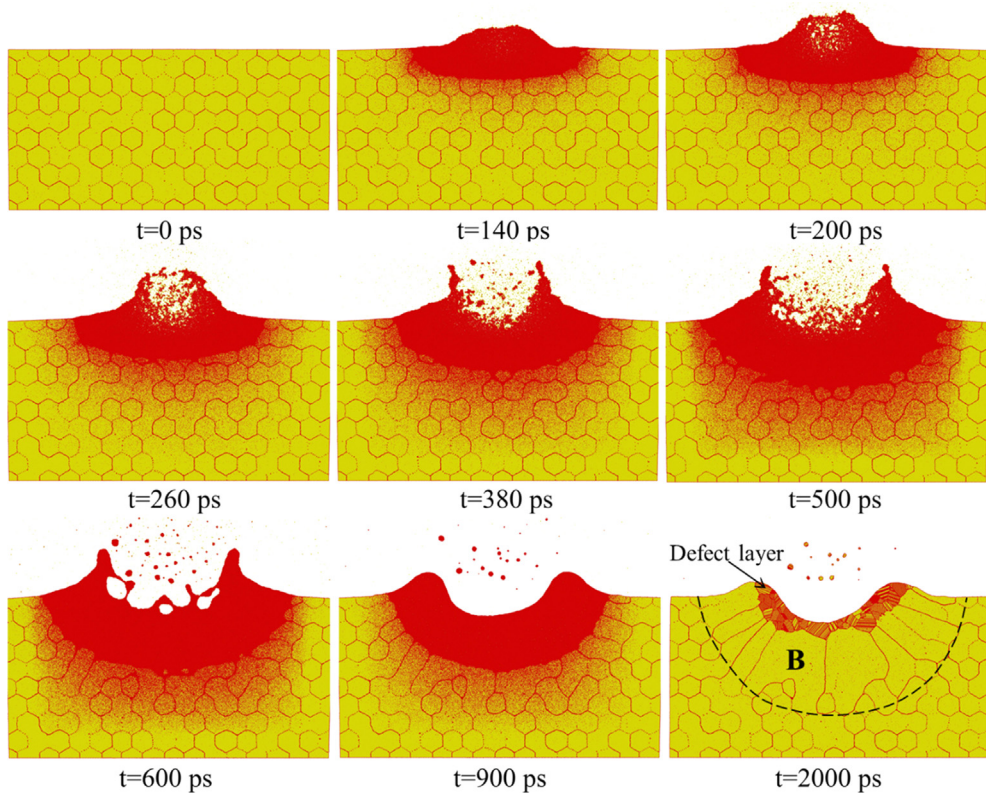


Fig. 8. Material removal process of polycrystalline copper with 10 nm grain size.

simplified as a regular hexagon whose side length represented the grain size. In the actual discharge process of EDM, most of the molten materials are not totally ablated and remain on the surface of discharge crater. The remaining materials are called the recast layer. Furthermore, under the recast layer, a heat affecting zone is also generated due to the quick heating and quenching process. The recast layer and the heat affecting zone are called to the denatured layer, which has significant influence on the material property of the components fabricated by EDM, such as the wear resistance, fatigue strength, hardness, corrosion resistance, etc [24]. The CSP method was also used to investigate the recast layer and heat affecting zone.

In Figs. 7 and 8, before the discharge, the red atoms ($CSP > 3$) stand for the grain boundary of the crystalline grain while the yellow atoms ($CSP < 3$) stand for the monocrystal copper inside the crystalline grain, as shown $t = 0$ ps. After the discharge was ignited, the region of red atoms increased around the discharge spot due to the thermal motion of atoms caused by the high temperature. As the discharge time went on, the region of red atoms expanded further. After the end of discharge, the electrode material cooled gradually and the molten material recrystallized into the crystal structure. Thus, the atoms state became ordered gradually and the red atoms became yellow atoms. From Figs. 7 and 8, after the discharge, it can be found that the crystalline grains under the discharge crater were changed greatly, such as the moment at 2000 ps. Thus, the changing area of crystalline grains can be approximately defined as the denatured layer, which was represented by the dotted black line. The zone under the dotted black line indicates that the discharge heat has very little influence on the material in this zone while the zone above the dotted black line means that the crystal structure of material in this zone has been changed by the discharge heat.

Furthermore, under the surface of discharge crater, the defect layer was generated, as shown in Figs. 6–8. The defect layer corresponds to the intensive defect structures generated during the solidification process of molten material. Especially, on the monocrystal copper, as shown in Fig. 6, the largest thickness of the defect layer was about 11.3 nm while the largest thicknesses of the polycrystalline copper with crystal size of 15 nm and 10 nm were about 16.7 nm and 19.2 nm, respectively. Moreover, under the discharge crater of the polycrystalline copper with the crystal size of 15 nm, eight new crystalline grains were generated and the largest crystalline grain has the area of 2114 nm^2 , as shown by A in Fig. 7. Under the discharge crater of the polycrystalline copper with the grain size of 10 nm, 11 new crystalline grains were generated and the largest crystalline grain has the area of

2689 nm^2 , as shown by B in Fig. 8. Fig. 9 shows the atom number of defect structures in defect layer. The simulation result demonstrates that atom number of defect structure in defect layer increased along with the decrease of the grain size of electrode material.

Thus, it can be concluded that compared with the monocrystal copper, discharge on the polycrystalline copper can generate much more defect structures and much larger denatured layer. Moreover, the smaller the grain size of polycrystalline copper, the more the defect structures and the larger the denatured layer will be. A plausible explanation for this result can be given as follows: according to the theory of metal solidification [25], after a nucleus is formed, the liquid atoms migrate to the surface of the nucleus and the grain is growing gradually. The growth of grain is the arrangement and stacking from the liquid atoms to the nucleus surface, which occurs at the interface of the solid and liquid phases. Thereby, the solid-liquid interface determines the growing patterns of grain. In the simulation of monocrystalline copper, the solid-liquid interface is between the monocrystalline and the liquid atoms, as shown in Fig. 6. In the MD simulation, the solidification of molten material is an ideal process without external interference, such as the temperature, pressure and impurity, and so forth. Thus, in the simulation of monocrystalline copper, the liquid atoms migrated to the solid-liquid interface and formed the monocrystalline, which is the face centered cubic structure (FCC), as shown in Fig. 6. But, in the simulation of polycrystalline copper, the solid-liquid interface is between the polycrystalline and liquid atoms, as shown in Figs. 7 and 8. On the solid-liquid interface, the grains have different crystal orientation. As a result, the liquid atoms migrated to the surface of these grains and formed new grains with different crystal orientations. Moreover, the smaller the grain size of polycrystalline copper, the more the newly formed grains were generated, as shown in Figs. 7 and 8. In the simulation of both monocrystalline and polycrystalline coppers, the defect layers were generated between the surface atoms and newly formed grains, where the atoms can't form the FCC structure. The more the newly formed grains, the more the defect atoms will be. From the above analysis, it can be concluded that smaller size of grain leads to more defects and larger denatured layer.

4. Conclusions

In the study, MD simulation of discharge process was conducted using a two-temperature model (TTM) to consider the influence of both the lattice vibration and free electrons on the thermal conduction simultaneously. Research findings were shown as follows:

- (1) Through the periodic boundary of MD simulation, a 2-D MD model was built so that the simulation scale could be reduced extremely. This 2-D sub-micrometer scale MD model based on TTM has successfully obtained a sub-micrometer scale discharge crater which was close to the smallest discharge crater reported. Moreover, the temperature distribution of the electrode material and the topography of the discharge crater demonstrate that this 2-D MD model based on TTM can simulate the discharge process more truly.
- (2) After the discharge was ignited, the pressure in the molten pool increased. Under the action of pressure, the molten materials swelled. When the pressure in the molten pool exceeded the binding force of atoms, the swelling molten materials broke open and molten materials departed from the molten pool. It can be concluded that this pressure generated inside the molten pool serves as one of the removal mechanisms of molten material in the discharge process of EDM.
- (3) Compared with the monocrystal copper, discharge on the polycrystalline copper can generate much more defect structures and larger denatured layer. Moreover, the smaller the grain size of polycrystalline copper, the more the defect structures and the larger the denatured layer will be.

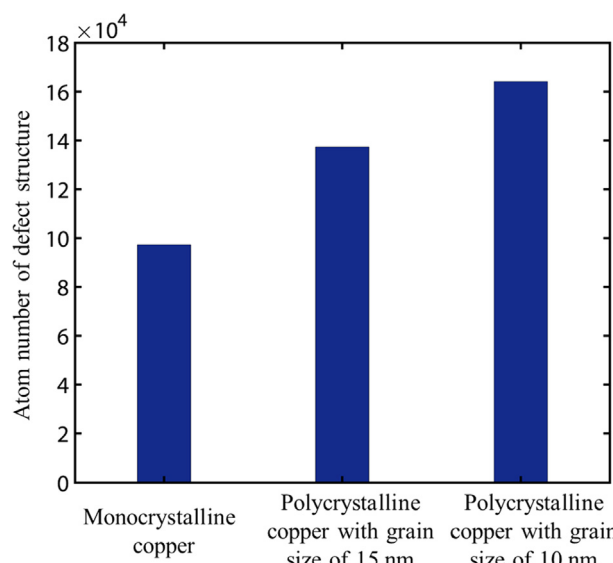


Fig. 9. Comparison of atom number of defect structure in defect layer.

Declaration of Competing Interest

The authors declare that they have no known competing financial interests or personal relationships that could have appeared to influence the work reported in this paper.

CRediT authorship contribution statement

Xiaoming Yue: Conceptualization, Investigation, Data curation, Writing - original draft. **Xiaodong Yang:** Supervision, Methodology, Writing - review & editing, Funding acquisition.

Acknowledgements

The authors would like to thank the National Natural Science Foundation of China (Youth Program, Grant No. 51905311) and (General Program, Grant No. 51875133), Natural Science Foundation of Jiangsu Province (BK2019041170), the Key Laboratory of High-efficiency and Clean Mechanical Manufacture at Shandong University (Ministry of Education), and the Fundamental Research Funds of Shandong University (2018TB030) for providing financial support for this research. The authors also would like to thank American Sandia National Laboratories for their free and open source software (Lammps).

References

- [1] M. Kunieda, B. Lauwers, K.P. Rajurkar, B.M. Schumacher, Advancing EDM through fundamental insight into the process, *Cirp. Ann.-Manuf. Technol.* 54 (2005) 599–622.
- [2] Y.B. Guo, A. Klink, F. Klocke, Multiscale modeling of sinking-EDM with gaussian heat flux via user subroutine, *Proc. Cirp.* 6 (2013) 438–443.
- [3] B. Izquierdo, J.A. Sanchez, S. Plaza, I. Pombo, N. Ortega, A numerical model of the EDM process considering the effect of multiple discharges, *Int. J. Mach. Tool Manuf.* 49 (2009) 220–229.
- [4] K. Saloniatis, A. Stournaras, P. Stavropoulos, G. Chryssolouris, Thermal modeling of the material removal rate and surface roughness for die-sinking EDM, *Int. J. Adv. Manuf. Technol.* 40 (2009) 316–323.
- [5] J. Tang, X. Yang, A novel thermo-hydraulic coupling model to investigate the crater formation in electrical discharge machining, *J. Phys. D Appl. Phys.* 50 (2017) 365301.
- [6] M. Foroutan, V.F. Naeini, M. Ebrahimi, Carbon nanotubes encapsulating fullerene as water nano-channels with distinctive selectivity: molecular dynamics simulation, *Appl. Surf. Sci.* 489 (2019) 198–209.
- [7] M. Shahabi, H. Raissi, Payload delivery of anticancer drug Tegafur with the assistance of graphene oxide nanosheet during biomembrane penetration: molecular dynamics simulation survey, *Appl. Surf. Sci.* 517 (2020) 146186.
- [8] V.-T. Nguyen, T.-H. Fang, Molecular dynamics simulation of abrasive characteristics and interfaces in chemical mechanical polishing, *Appl. Surf. Sci.* 509 (2020) 144676.
- [9] S. Shimada, H. Tanaka, N. Mohri, H. Takezawa, Y. Ito, R. Tanabe, Molecular dynamics analysis of self-sharpening phenomenon of thin electrode in single discharge, *J. Mater. Process. Technol.* 149 (2004) 358–362.
- [10] X.D. Yang, J.W. Guo, X.F. Chen, M. Kunieda, Molecular dynamics simulation of the material removal mechanism in micro-EDM, *Precis. Eng.* 35 (2011) 51–57.
- [11] X. Yang, X. Han, F. Zhou, M. Kunieda, Molecular dynamics simulation of residual stress generated in EDM, *Proc. Cirp.* 6 (2013) 432–437.
- [12] X.M. Yue, X.D. Yang, Molecular dynamics simulation of material removal process and crystal structure evolution in EDM with discharge on different crystal planes, *Int. J. Adv. Manuf. Technol.* 92 (2017) 3155–3165.
- [13] X.M. Yue, X.D. Yang, Molecular dynamics simulation of machining properties of polycrystalline copper in electrical discharge machining, *P I Mech. Eng. B* 233 (2019) 371–380.
- [14] X.M. Yue, X.D. Yang, Molecular dynamics simulation of the material removal process and gap phenomenon of nano EDM in deionized water, *RSC Adv.* 5 (2015) 66502–66510.
- [15] G.J. Zhang, J.W. Guo, W.Y. Ming, Y. Huang, X.Y. Shao, Z. Zhang, Study of the machining process of nano-electrical discharge machining based on combined atomistic-continuum modeling method, *Appl. Surf. Sci.* 290 (2014) 359–367.
- [16] M. Kunieda, A. Hayasaka, X.D. Yang, S. Sano, I. Araie, Study on nano EDM using capacity coupled pulse generator, *Cirp. Ann.-Manuf. Technol.* 56 (2007) 213–216.
- [17] X.D. Yang, C.W. Xu, M. Kunieda, Miniaturization of WEDM using electrostatic induction feeding method, *Precis. Eng.* 34 (2010) 279–285.
- [18] H. Takeuchi, M. Kunieda, Effects of volume fraction of bubbles in discharge gap on machining phenomena of EDM, *Proceedings of the 15th International Symposium on Electromachining*, 2007, pp. 63–68.
- [19] Sandia Corporation. LAMMPS, <http://lammps.sandia.gov/>, 2017 (accessed 13 November 2017).
- [20] S.M. Foiles, M.I. Baskes, M.S. Daw, Embedded-atom-method functions for the Fcc metals Cu, Ag, Au, Ni, Pd, Pt, and their alloys, *Phys. Rev. B* 33 (1986) 7983–7991.
- [21] A. Kojima, W. Natsu, M. Kunieda, Spectroscopic measurement of arc plasma diameter in EDM, *Cirp. Ann.-Manuf. Technol.* 57 (2008) 203–207.
- [22] D.M. Duffy, A.M. Rutherford, Including the effects of electronic stopping and electron-ion interactions in radiation damage simulations, *J. Phys.: Condens. Matter* 19 (2006) 016207.
- [23] C.L. Kelchner, S.J. Plimpton, J.C. Hamilton, Dislocation nucleation and defect structure during surface indentation, *Phys. Rev. B* 58 (1998) 11085–11088.
- [24] Y.S. Liao, J.T. Huang, Y.H. Chen, A study to achieve a fine surface finish in Wire-EDM, *J. Mater. Process. Technol.* 149 (2004) 165–171.
- [25] W. Kurz, D.J. Fisher, Fundamentals of Solidification, Atom transfer at the solid/liquid interface, Trans Tech Publications Ltd, Zurich, 1998, pp. 21–34.